CELL BIOLOGY

PKA Cα subunit mutation triggers caspase-dependent RIIβ subunit degradation via Ser^{114} phosphorylation

Isabel Weigand[1], Cristina L. Ronchi[1,2,3], Jens T. Vanselow[4,5], Kerstin Bathon[6], Kerstin Lenz[1], Sabine Herterich[7], Andreas Schlosser[4], Matthias Kroiss[1,8], Martin Fassnacht[1,7,8]*, Davide Calebiro[2,6,9], Silviu Sbiera[1,7]*

Mutations in the *PRKACA* gene are the most frequent cause of cortisol-producing adrenocortical adenomas leading to Cushing's syndrome. *PRKACA* encodes for the catalytic subunit α of protein kinase A (PKA). We already showed that *PRKACA* mutations lead to impairment of regulatory (R) subunit binding. Furthermore, *PRKACA* mutations are associated with reduced RIIβ protein levels; however, the mechanisms leading to reduced RIIβ levels are presently unknown. Here, we investigate the effects of the most frequent *PRKACA* mutation, L206R, on regulatory subunit stability. We find that Ser^{114} phosphorylation of RIIβ is required for its degradation, mediated by caspase 16. Last, we show that the resulting reduction in RIIβ protein levels leads to increased cortisol secretion in adrenocortical cells. These findings reveal the molecular mechanisms and pathophysiological relevance of the R subunit degradation caused by *PRKACA* mutations, adding another dimension to the deregulation of PKA signaling caused by *PRKACA* mutations in adrenal Cushing's syndrome.

INTRODUCTION

Cushing's syndrome (CS), a severe condition characterized by endogenous cortisol excess, is associated with increased morbidity and mortality. Adrenocorticotropic hormone (ACTH)–independent CS is most often caused by benign cortisol-producing adrenal adenomas (CPAs), 30 to 67% of which carry activating mutations in the *PRKACA* gene encoding the catalytic subunit α of protein kinase A (PKA) (*1*–*4*).

In its inactive form, PKA is a heterotetramer that consists of two catalytic (C) and two regulatory (R) subunits (*5*). Both catalytic and regulatory subunits exist in several isoforms, three catalytic (α, β, and γ) and four regulatory (Iα, Iβ, IIα, and IIβ) subunit isoforms, each encoded by a separate gene (*6*) and expressed differentially throughout tissues (*7*). While the C subunits catalyze the phosphorylation of a range of target substrates, the R subunits inhibit this catalytic activity in the absence of cyclic adenosine 5′-monophosphate (cAMP). R subunits confer differential localization of the tetrameric complex to different subcellular compartments. The latter is achieved via interaction with a family of scaffolding proteins known as A-kinase anchoring proteins (AKAPs) (*7*). Within the heterotetramer, two short sequences of the R subunits, called inhibitory sequences, occupy the catalytic clefts of the C subunits, thus preventing the binding of PKA substrates. While the inhibitory sequences of type I R subunits function as pseudosubstrates, those of type II R subunits contain a serine residue that can be phosphorylated and, thus, function as proper substrates (*8*). Upon binding of cAMP, the R subunits undergo a conformational change that reduces their affinity for C subunits, leading to the release and activation of the C subunits (*9*).

Most of the mutations in the catalytic α subunit of PKA (*PRKACA*) found in CPAs lie in a hotspot at the interface between R and C subunits (*4*, *10*, *11*). Several of these *PRKACA* mutations were shown to hamper the formation of the inactive PKA tetrameric complex (*4*, *10*, *11*), therefore rendering PKA constitutively active. In addition, three *PRKACA* mutations were demonstrated to alter substrate specificity, leading to, among others, hyperphosphorylation of histone H1.4 (*11*). Earlier research has shown that certain CPAs have reduced levels of the R subunit IIβ (RIIβ) (*12*), and we could recently link this cellular RIIβ protein loss to *PRKACA* mutations (*13*). However, to date, the mechanisms leading to this loss and both its molecular and functional consequences remain elusive. In this study, we provide functional evidence that *PRKACA* L206R regulate RIIβ degradation and show that this degradation is mediated by caspases. RIIβ degradation is a result of the serine residue within its inhibitory site being phosphorylated. We further demonstrate altered RIIβ protein–binding partners in the presence or absence of the L206R mutation.

RESULTS

PRKACA L206R leads to caspase-mediated RIIβ degradation

We recently have shown significantly reduced RIIβ protein expression in *PRKACA*-mutated CPAs compared with *PRKACA*–wild-type (WT) CPAs (*13*). At that time, we could neither demonstrate a direct causative role for Cα mutations on the reduction in RIIβ levels nor its functional consequences. To answer these questions, we silenced RIIβ via small interfering RNA (siRNA) in the steroidogenic adrenocortical cell line NCI-H295R. RIIβ silencing led to a significant increase in cortisol secretion (fig. S1), while the secretion of several other steroid hormones was unchanged (table S1). We next tested the stability of RIIβ and other R subunits in the presence of the Cα L206R mutant or WT Cα in the same cells. In NCI-H295R

[1]Division of Endocrinology and Diabetes, Department of Internal Medicine I, University Hospital, University of Würzburg, 97080 Würzburg, Germany. [2]Institute of Metabolism and System Research, University of Birmingham, Edgbaston, Birmingham B15 2TT, UK. [3]Centre for Endocrinology, Diabetes and Metabolism, Birmingham Health Partners, Edgbaston, Birmingham B15 2TT, UK. [4]Rudolf-Virchow-Center for Integrative and Translational Bioimaging, University of Würzburg, 97080 Würzburg, Germany. [5]Department of Chemical and Product Safety, German Federal Institute of Risk Assessment (BfR), 10589 Berlin, Germany. [6]Institute of Pharmacology and Toxicology and Bio-Imaging Center, University of Würzburg, 97080 Würzburg, Germany. [7]Central Laboratory, University Hospital Würzburg, 97080 Würzburg, Germany. [8]Comprehensive Cancer Center Mainfranken, University of Würzburg, 97080 Würzburg, Germany. [9]Centre of Membrane Proteins and Receptors (COMPARE), Universities of Nottingham and Birmingham, Birmingham B15 2TT, UK.
*Corresponding author. Email: fassnacht_m@ukw.de (M.F.); sbiera_s@ukw.de (S.S.)

cells transiently transfected with Cα WT, Cα L206R, or empty vector as control in combination with RIIβ-FLAG, RIIβ levels were only stable in the presence of Cα WT (1 ± 0.12) but not in the presence of Cα L206R (0.04 ± 0.02) or empty vector (0.01 ± 0.01) ($P < 0.05$; Fig. 1, A and B). RIIβ degradation in the presence of Cα L206R was restricted to adrenocortical cells, as it was also observed in two other human adrenocortical carcinoma (ACC) cell lines: CU-ACC1 and CU-ACC2 (fig. S2, A to D) (*14*), but not in the embryonic kidney human embryonic kidney (HEK) 293T cells, neither in transiently transfected (fig. S2, E and F) nor in cells harboring the L206R point mutation introduced via CRISPR-Cas9 gene editing (fig. S2, G to I). Furthermore, RIIβ degradation was not observed in the human melanoma cell lines SK-MEL-28 and A375 either (fig. S2, J to M). Pharmacological inhibition of proteasome degradation with MG132 prevented the degradation of RIIβ in the absence but not in the presence of the L206R mutant (Fig. 1, A and B). In contrast to RIIβ, RIα was stable except in the absence of exogenous catalytic subunits (Fig. 1, A and B). Pharmacological inhibition of the proteasome protected RIα from degradation in the absence of exogenous catalytic subunit (Fig. 1, D and E). These results were obtained at similar expression levels of the transfected WT and L206R Cα subunits (Fig. 1, C and F). Pulse-chase experiments revealed comparable translation of RIIβ in the presence of either Cα WT or L206R (Fig. 1G). To identify the type of protease responsible for RIIβ degradation, cells transfected with Cα L206R were treated for 6 hours with different protease inhibitors, and RIIβ protein expression was monitored. Among the tested inhibitors, only the pan-caspase inhibitor Z-VAD-FMK was able to partially prevent RIIβ degradation in the presence of the L206R mutant (Fig. 1, H and I and fig. S3, A and C) while RIIβ levels remained largely unaffected by caspases inhibition in Cα WT conditions (Fig. 1, J and K).

PKA activity protects RIIβ from degradation

To investigate whether PKA activity influences RIIβ stability, we performed similar experiments in NCI-H295R cells in the presence of the PKA activator 8-Br-cAMP or the PKA inhibitor H89. Unexpectedly, 8-Br-cAMP treatment significantly increased RIIβ protein levels in the presence of the L206R Cα mutant compared with vehicle control (Fig. 2, A and B), while H89 reduced RIIβ protein levels even further (Fig. 2, A and B). A similar trend was observed with RIα, although the differences did not reach statistical significance (Fig. 2, C and D). To distinguish between the alternative possibilities that the protective effects of 8-Br-cAMP might be due to either its occupation of the cAMP-binding sites of the RIIβ subunit or the consequent stimulation of PKA activity, we additionally tested the effects of two cAMP analogs that preferentially bind RI (Rp-8-Br-cAMPs) or RII (Rp-8-PIP-cAMPs) subunits but act as competitive PKA inhibitors (*15*). Neither inhibitory cAMP analog protected RIIβ from degradation in the presence of the L206R mutant (Fig. 2, E and F) or affected RIα stability (Fig. 2, G and H). In addition, cotreatment with the PKA inhibitor H89 (0.05 ± 0.03) fully prevented the protective effect of 8-Br-cAMP (1 ± 0.07) on RIIβ degradation ($P < 0.001$) (Fig. 2, I and J). Similar results were obtained with PKI, a synthetic peptide inhibitor of PKA (fig. S5, A and B). Moreover, a kinase dead variant (K73H) (*16*) of the L206R mutant (Cα K73H/L206R) resulted in incomplete RIIβ degradation (fig. S5, C and D). These results suggest that specific L206R activity leads to RIIβ degradation and that 8-Br-cAMP activates the endogenous, WT PKA that protects RIIβ from degradation in the presence of the L206R mutant.

Phosphorylation of RIIβ by Cα L206R tags RIIβ for degradation

We then investigated the phosphorylation of RIIβ at Ser^{114} under the same experimental conditions. We found that the levels of RIIβ phosphorylation (p-RIIβ) decreased upon PKA activation with 8-Br-cAMP, suggesting that RIIβ phosphorylation might be associated with its degradation (Fig. 2I). Because the substrate RIIβ is degraded in the presence of Cα L206R but the pseudosubstrate RIα is not, we asked whether the phosphorylation of RIIβ is the factor affecting its stability. To test this, RIIβ constructs were generated in which Ser^{114} (S114) was mutated to either alanine (A) (RIIβ S114A), as found in RIα, or to the phosphomimetic amino acid aspartic acid (D) (RIIβ S114D). In addition, we tested two chimeric constructs in which either the whole inhibitory sequence (RIIβ inhibitory) or the same sequence plus additional flanking amino acids (RIIβ inhibitory extended) of RIIβ were replaced with the corresponding sequences found in RIα. In parallel, we tested symmetrical RIα constructs carrying a serine (RIα A99S) or the corresponding replacements from RIIβ (RIα inhibitory, RIα inhibitory extended) (Fig. 3A). In the presence of the Cα L206R mutant, all R subunit constructs having either a serine or aspartic acid within their inhibitory site were detected at low levels, while all constructs having an alanine within their inhibitory site were present at levels comparable to WT (Fig. 3, B and C) (phosphorylatable R subunits versus nonphosphorylatable R subunits 0.6 ± 0.2 versus 7.6 ± 0.9, $P < 0.0001$). In addition, all phosphorylatable RIIβ constructs could be rescued by 8-Br-cAMP stimulation (Fig. 3, B and C). RIIβ was predominantly phosphorylated in its WT form without 8-Br-cAMP treatment (Fig. 3, B and D). In Cα WT cotransfections, all R subunit constructs were expressed at similar levels (fig. S4, A and B). In an attempt to increase the amount of phosphorylated RIIβ, phosphatases were inhibited with tautomycetin. Tautomycetin treatment alone had no effect on RIIβ protein levels, but when combined with the PKA activator 8-Br-cAMP, RIIβ levels were reduced, although not significantly, compared with 8-Br-cAMP treatment alone (Fig. 3, E and F). These results indicate that phosphorylation of the serine residue within R subunit inhibitory sequences is involved in its degradation.

RIIβ interacts with golgin A3 in the presence of Cα L206R

Because PKA interacts via its R subunits with AKAPs and other proteins to form signaling complexes, we hypothesized that the degradation of RIIβ observed in the presence of the L206R mutation might involve changes in the proteins interacting with RIIβ. To test this hypothesis, we transfected the adrenocortical cell line NCI-H295R with Cα WT or Cα L206R and RIIβ-FLAG and performed immunoprecipitation with an anti-FLAG antibody in the absence or presence of 8-Br-cAMP. Regardless of the PKA mutation status, nano–liquid chromatography–tandem mass spectrometry (nanoLC-MS/MS) showed comparable enrichment of proteins in either 8-Br-cAMP or unstimulated conditions (Fig. 4, A and B). Golgin A3 was among the proteins consistently identified to bind RIIβ only in the presence of the Cα L206R mutant (Fig. 4B). The specificity of this interaction was subsequently verified by coimmunoprecipitation (co-IP) and Western blotting (WB) and confirmed to occur only in the presence of Cα L206R and in unstimulated conditions [L206R (1.8 ± 0.2) compared with 8-Br-cAMP treatment (0.07 ± 0.06) and compared with WT in vehicle-treated (0.006 ± 0.004) versus 8-Br-cAMP–treated cells (0.04 ± 0.02); $P < 0.01$] (Fig. 4, C and D). Because this is the only condition in which RIIβ is degraded, we reasoned

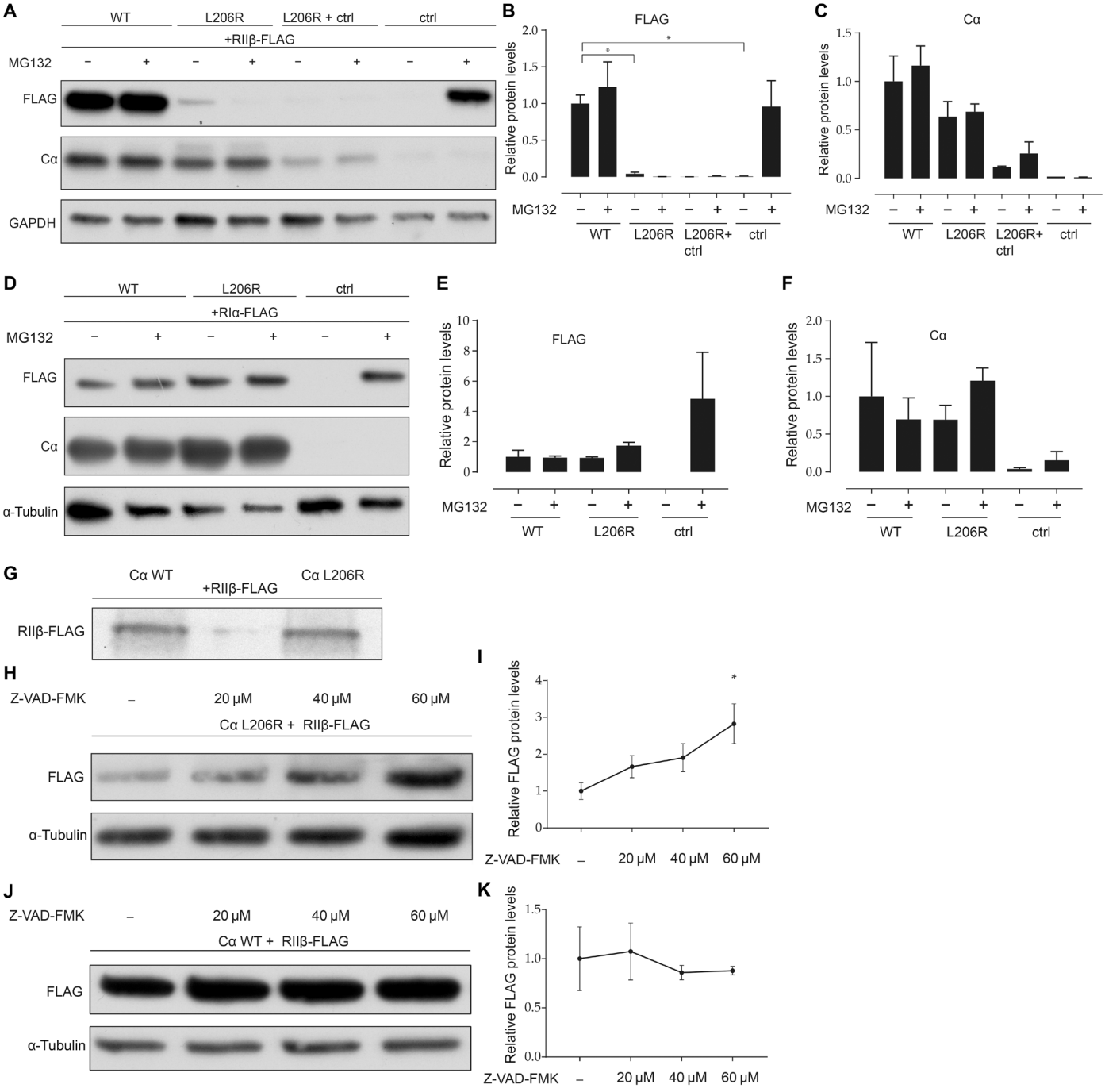

Fig. 1. RIIβ is posttranslationally degraded by caspases in the presence of Cα L206R. (**A**) WB of transiently transfected NCI-H295R cells. RIIβ protein levels are stable when cotransfected with Cα WT but not when cotransfected with different amounts of Cα L206R or ctrl vector. Proteasome inhibition with MG132 had only protecting effects in ctrl-transfected cells (A and **B**). Cα protein levels depended on the amount of transfected DNA and were slightly but not significantly fewer in L206R compared with WT-transfected cells (**C**). RIα protein levels were stably independent of the Cα mutational status but unstable when cotransfected with ctrl vector (**D** and **E**). MG132 protected from proteasomal degradation. Cα transfection levels were comparable (**F**). Representative pulse experiment reveals similar amounts of newly translated RIIβ independent of the Cα mutational status (**G**). Increasing concentrations of the pan-caspase inhibitor Z-VAD-FMK significantly increased RIIβ protein levels in Cα L206R–transfected cells (**H** and **I**), while there were no effects on RIIβ Cα WT–transfected cells (**J** and **K**). One-way analysis of variance (ANOVA) with Tukey's post hoc test was performed to determine significant differences between samples. *$P < 0.05$, means ± SEM.

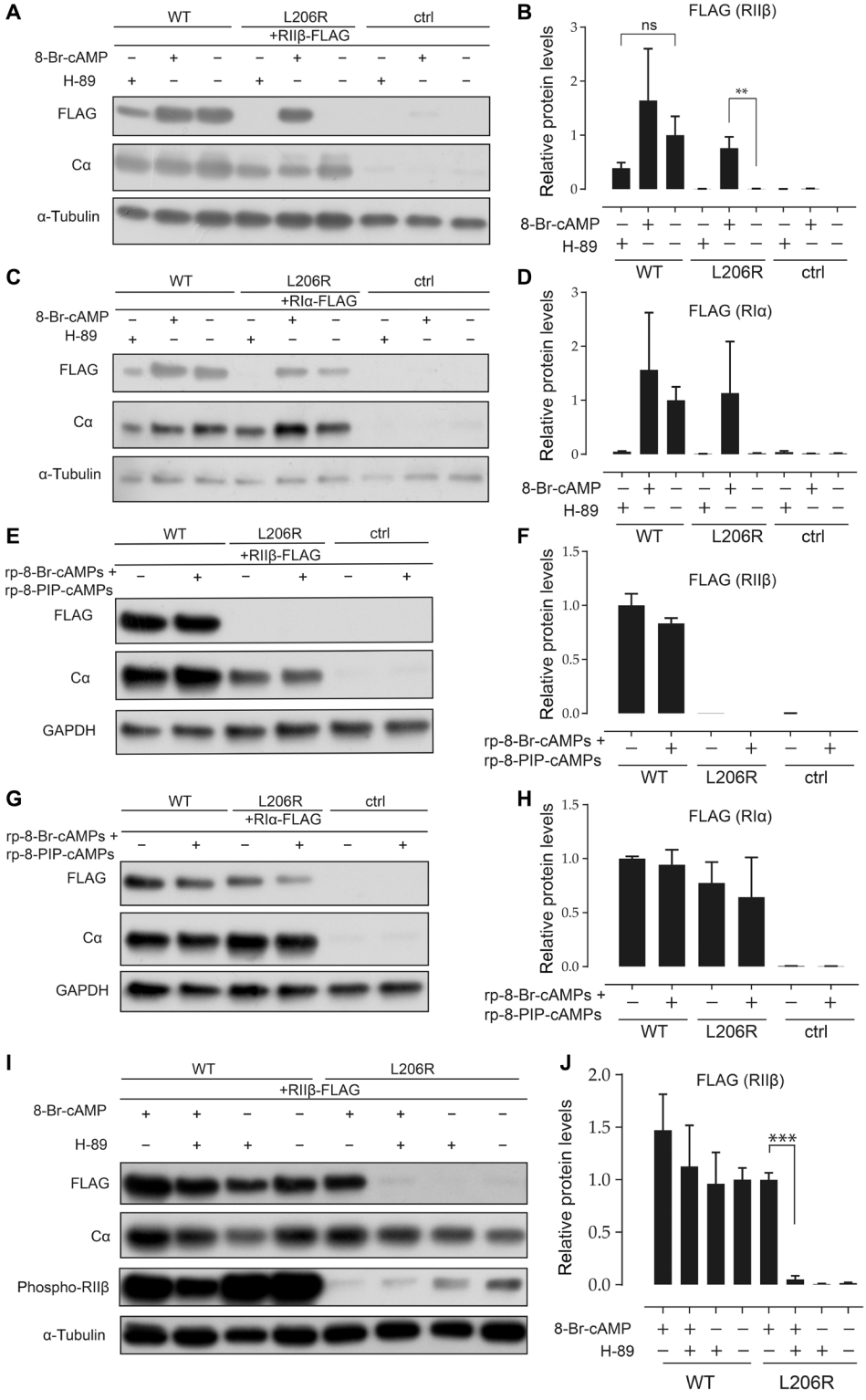

Fig. 2. Activation of PKA signaling protects RIIβ from Cα L206R–induced degradation. PKA activation with the cAMP analog 8-Br-cAMP significantly rescued RIIβ in Cα L206R–transfected cells, while inhibition of PKA with H-89 did not (**A** and **B**). Neither PKA activation nor inhibition had a significant effect on RIα protein levels in the presence of Cα L206R (**C** and **D**), while H-89 treatment even reduced RIα (as RIIβ) protein levels even in Cα WT conditions (B and C). Inhibitory cAMP analogs were not able to protect RIIβ protein levels in Cα L206R cells, not in mock transfected cells (**E** and **F**), while these inhibitors had no effect on RIα protein stability (**G** and **H**). Simultaneous activation with a cAMP analog and inhibition with H-89 showed superior effectivity of inhibition over activation (**I** and **J**). In addition, all RIIβ to be rescued was unphosphorylated (I). One-way ANOVA with Tukey's post hoc test was performed to determine significant differences between samples. ns, not significant. $^{**}P < 0.01$, $^{***}P < 0.001$, means ± SEM.

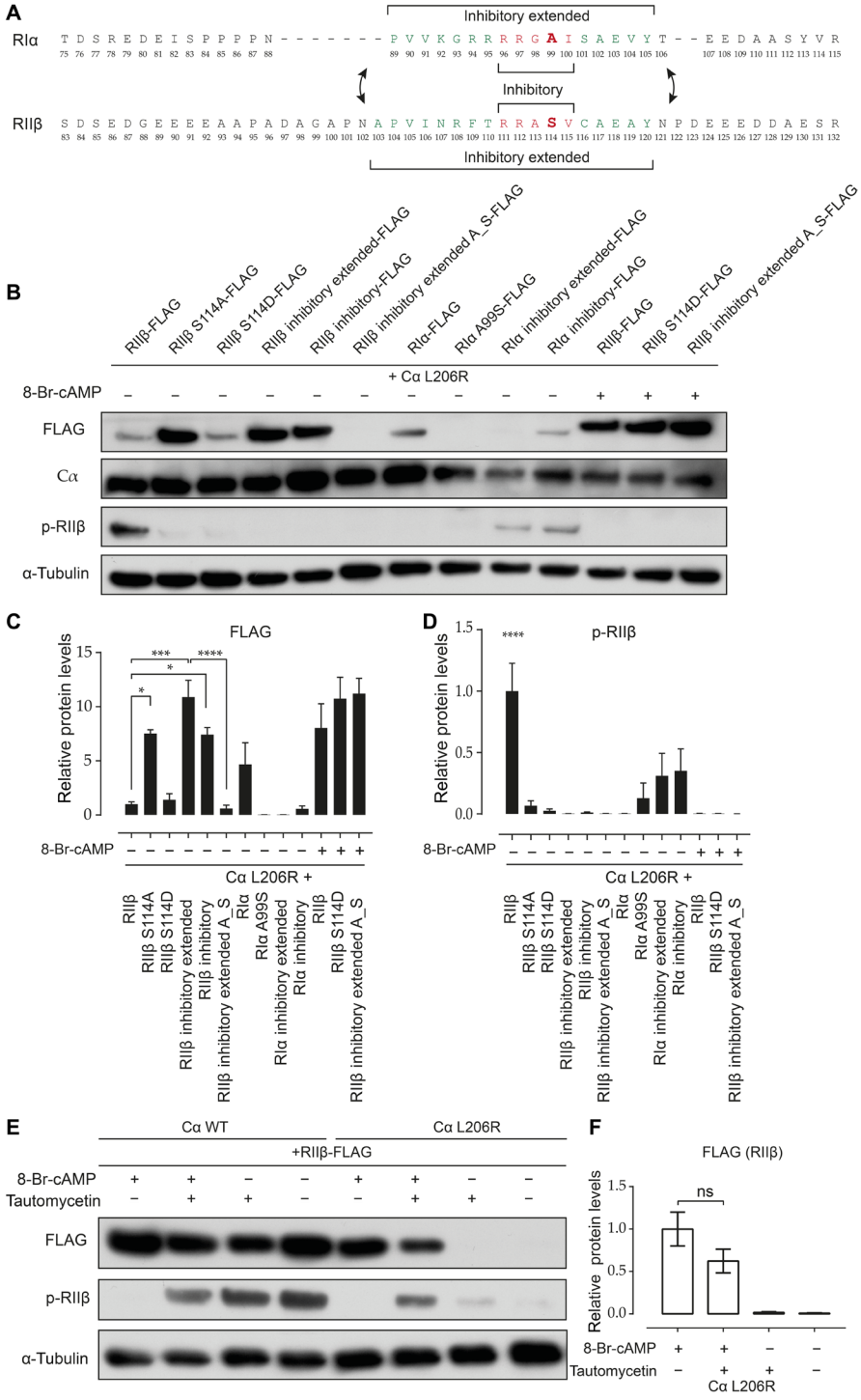

Fig. 3. Phosphorylation of RIIβ within its inhibitory site tags it for caspase-mediated cleavage. Sequences spanning the inhibitory sites (red) of both RIα (above) and RIIβ (below). Either alanine-99 (A99) in the case of RIα or Ser^{114} (S114) in the case of RIIβ is highlighted in bold. Additional amino acids mutated in the chimera constructs are shown in green (**A**). Exemplary WB results of NCI-H295R cells transfected with Cα L206R, RIIβ WT, RIα WT, and several forms of both regulatory subunits. RIIβ WT, RIIβ S114D, and the RIIβ-inhibitory extended A_S were additionally treated with 8-Br-cAMP (**B**). Densitometric analysis of WB FLAG bands, normalized to loading control and compared with untreated RIIβ WT. Analysis of three independent replicates (means ± SEM) (**C**). Densitometric analysis of WB of phosphorylation of R subunits, normalized to loading control and compared with untreated RIIβ WT. Analysis of three independent replicates (means ± SEM) (**D**). One-way ANOVA with Tukey's post hoc test was performed to determine significant differences between samples. *$P < 0.05$, ***$P < 0.001$, and ****$P < 0.0001$. Exemplary WB results of adrenocortical NCI-H295R cells transfected with RIIβ and Cα WT or L206R and treated with tautomycetin, 8-Br-cAMP, or both (**E**). Densitometric analysis of WB FLAG-bands, normalized to loading control and compared with L206R 8-Br-cAMP–treated samples. Analysis of eight independent replicates (means ± SEM). One-way ANOVA followed by Tukey's post hoc test was performed to determine significant differences between samples (**F**).

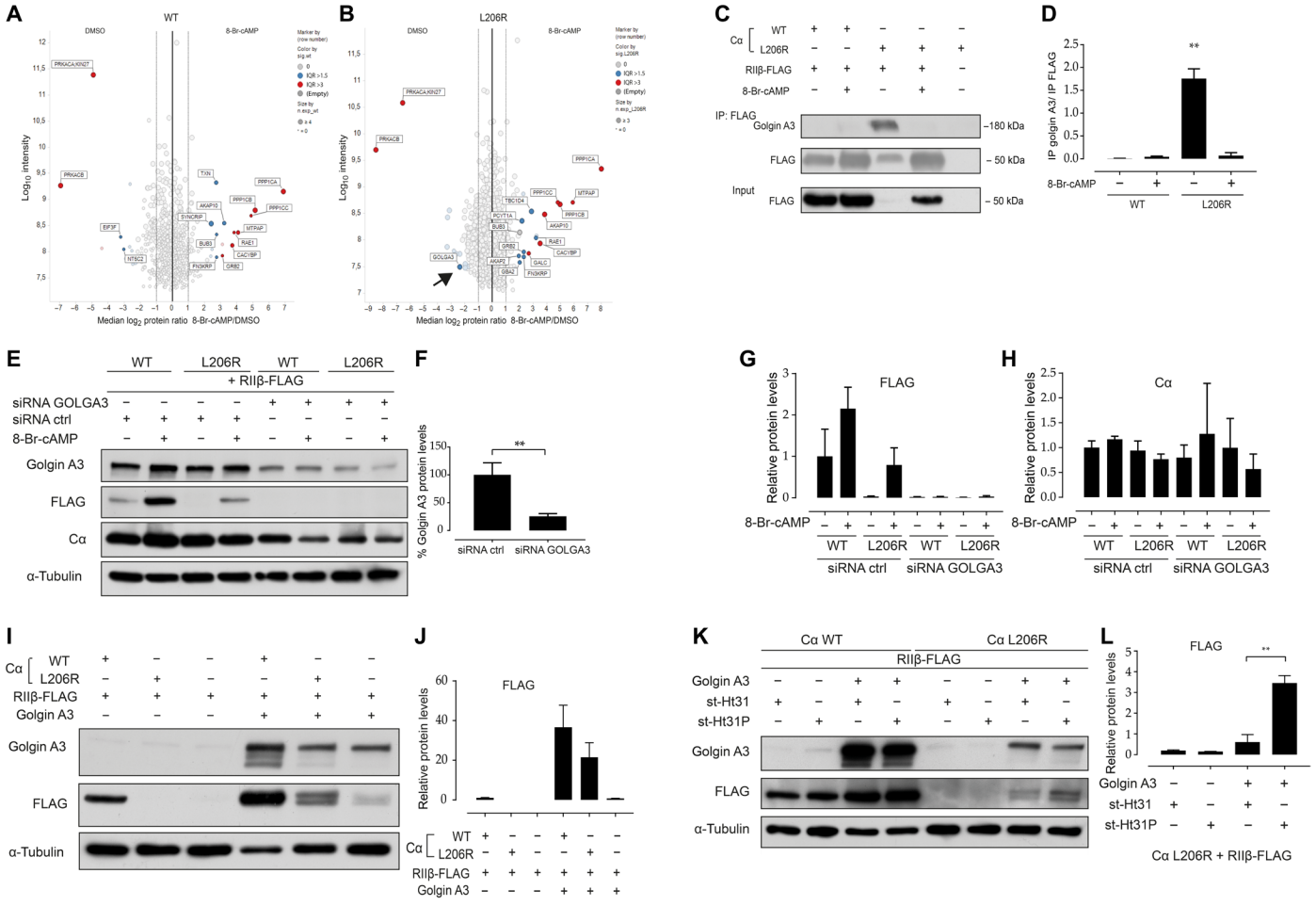

Fig. 4. LC-MS/MS results in Cα WT– and Cα L206R-transfected NCI-H295R cells and the effects of *GOLGA3* knockdown on RIIβ protein levels. (**A**) Proteins interacting with RIIβ in Cα WT samples without stimulation (left-hand side) and after 8-Br-cAMP stimulation (right-hand side). (**B**) Proteins interacting with RIIβ in Cα L206R samples without stimulation (left-hand side) and after 8-Br-cAMP stimulation (right-hand side). Each dot represents one protein, and the size of the dots represents the number of replicates, in which the proteins were identified in the single conditions. The intensity on the *y* axis represents the summed peptide intensities for each protein. Legend: Highlighted dots, significantly changed (Benjamini-Hochberg adjusted $P \leq 0.02$); color of dots represents highly significant changed protein interactions according to box-plot outliers: red, with interquartile range IQR >3; blue, with IQR >1.5. Only true RIIβ interaction partners that differed according to the two treatments are specified. $n = 4$ (WT), $n = 3$ (L206R). DMSO, dimethyl sulfoxide. (**C**) RIIβ-GOLGA3 (golgin A3) interaction only in the presence of Cα L206R was verified by WB. (**D**) Densitometric analysis of two independent replicates (means ± SEM). One-way ANOVA followed by Tukey's post hoc test was performed to determine significant differences between samples. $^{**}P < 0.01$. (**E**) Knockdown of *GOLGA3* leads to reduced RIIβ protein levels independent of the Cα mutation status. Densitometric analysis of (**F**) golgin A3, (**G**) FLAG, and (**H**) Cα protein levels. (**I**) Overexpression of golgin A3 was able to rescue RIIβ from degradation. (**J**) Densitometric analysis of RIIβ-FLAG levels. (**K**) Interrupting binding of R subunits to AKAPs with the peptide st-Ht31 significantly reduced RIIβ rescue by golgin A3 compared with control peptide st-Ht31P. (**L**) Densitometric analysis of RIIβ-FLAG levels. One-way ANOVA followed by Tukey's post hoc test was performed to determine significant differences between samples. $^{**}P < 0.01$ (means ± SEM).

that this interaction might be involved in RIIβ degradation. To test this hypothesis, we silenced golgin A3 with siRNA, which led to a significant reduction in golgin A3 protein levels to less than 30% [siRNA control (ctrl): 100 ± 21 versus siRNA golgin A3: 25 ± 5] (Fig. 4, E and F). Unexpectedly, reduction in golgin A3 led to complete loss of RIIβ-FLAG protein levels, independently of the presence of either Cα WT/L206R or 8-Br-cAMP stimulation (Fig. 4, E and G), while Cα protein levels themselves were largely unaffected (Fig. 4, E and H). Conversely, overexpression of golgin A3 markedly increased RIIβ protein levels (L206R: 0.007 ± 0.002 versus L206R + golgin A3: 21.5 ± 7.3) (Fig. 4, I and J). To test whether golgin A3 is a putative AKAP, R subunit AKAP binding was disrupted with the st-Ht31 peptide (*17*). In this condition, significantly more RIIβ was degraded (0.6 ± 0.4) compared with cells treated with the st-Ht31P control peptide, which does not disrupt binding to AKAPs (3.5 ± 0.4) ($P < 0.01$; Fig. 4, K and L). These results indicate that golgin A3 is an AKAP and that this interaction stabilizes RIIβ.

CASP16P is up-regulated in *PRKACA*-mutated CPAs and NCI-H295R cells

In an attempt to identify the caspase involved in RIIβ degradation, we mined an available RNA-sequencing dataset comprising different adrenocortical tumor entities (*18*), including 52 adrenal adenomas [CPA Cα WT and CPA Cα mutated, endocrine inactive adenomas (EIAs)] and 7 adrenocortical carcinomas (ACCs). Only one caspase gene was found to be differentially expressed between WT ($n = 37$) and *PRKACA*-mutated CPA ($n = 6$) samples, which was *CASP16P*. *CASP16P* mRNA expression was higher in *PRKACA*-mutated compared

with *PRKACA* WT samples (FPKM 2.4 ± 0.3 versus 0.7 ± 0.2; $P = 0.08$) but also compared with ACC samples (−0.7 ± 0.6; $P < 0.005$) and normal adrenal glands (nAGs) (−0.1 ± 0.2; $P < 0.05$) (Fig. 5A). To confirm these results, we performed a reverse transcription quantitative polymerase chain reaction (RT-qPCR) analysis of an independent cohort of 12 nAGs and 34 benign adrenocortical tumors and added aldosterone-producing adenomas (APAs) as an additional control group. Again, *CASP16P* mRNA expression was higher in *PRKACA*-mutated CPA (0.1 ± 0.03) compared with *PRKACA* WT CPA (0.04 ± 0.01; $P = 0.1$), EIA (0.008 ± 0.01; $P = 0.008$), APA

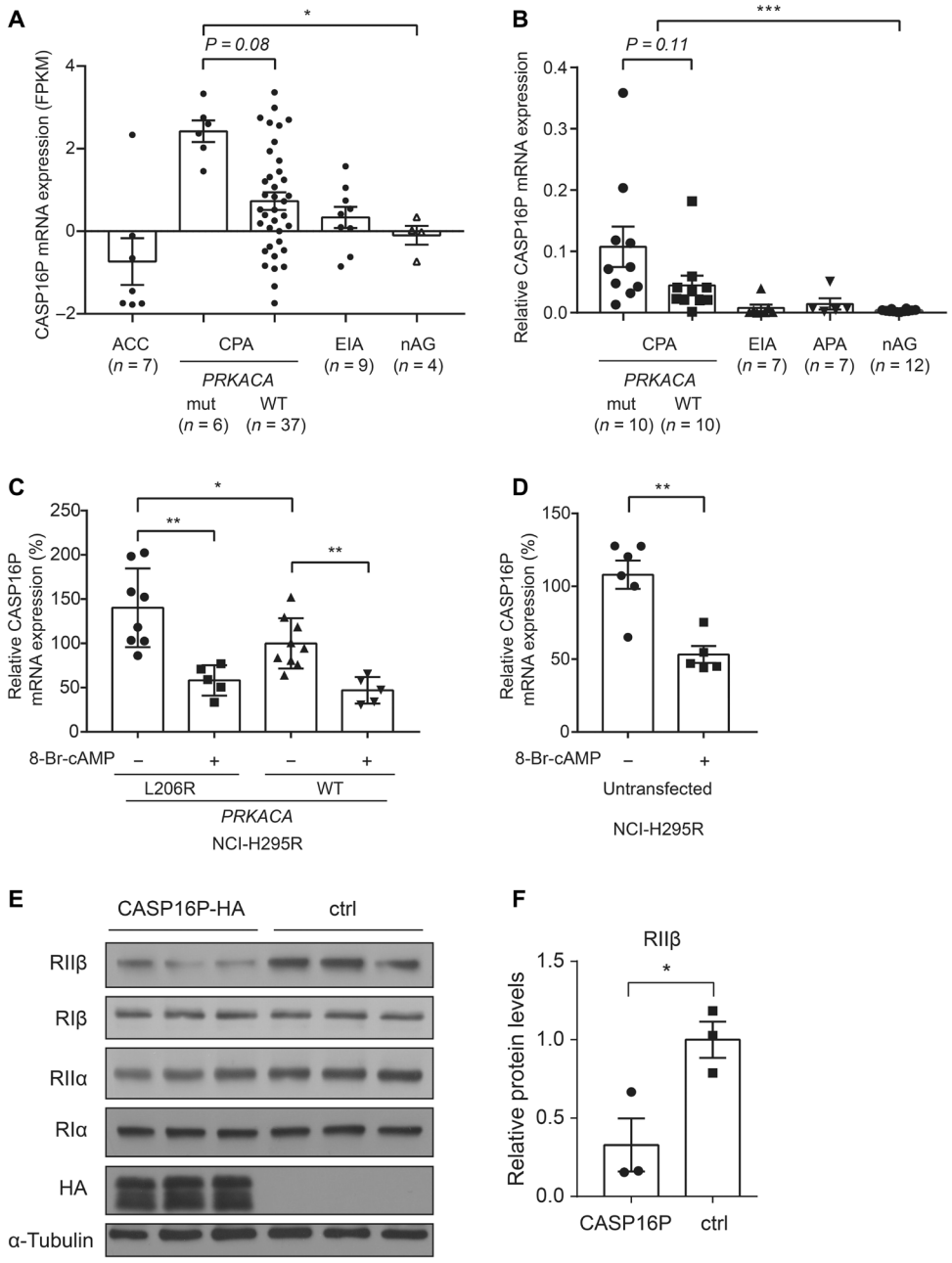

Fig. 5. Elevated levels of CASP16P mRNA in *PRKACA*-mutated CPAs. Gene expression profile by RNA sequencing of different adrenocortical tumor entities and normal tissue revealed significantly higher CASP16P RNA levels in CPA compared with nAG. *PRKACA*-mutated CPA had highest CASP16P mRNA expression (**A**). CASP16P mRNA expression was validated by qPCR in another set of adrenocortical adenomas and normal tissues. Again, *PRKACA*-mutated CPA had highest CASP16P mRNA expression (**B**). When NCI-H295R cells were transfected with Cα L206R, CASP16P mRNA levels were higher compared with cells transfected with Cα WT, and 8-Br-cAMP treatment significantly reduced CASP16P mRNA in both WT- and L206R-transfected cells (**C**). 8-Br-cAMP further reduced CASP16P mRNA levels in untransfected NCI-H295R cells (**D**). CASP16P-HA overexpression in NCI-H295R cells significantly reduced levels of endogenous RIIβ, while all other PKA regulatory subunits remained largely unaffected (**E**). Densitometric analysis of RIIβ levels with and without CASP16P overexpression (**F**). CPA, cortisol-producing adenoma; APA, aldosterone-producing adenoma; FPKM, fragments per kilobase million. Kruskal-Wallis test was performed to determine significant differences in patient-derived samples (A and B). One-way ANOVA (C) and nonparametric *t* test (D and F) were performed to determine significant differences between cell culture samples, $^*P < 0.05$, $^{**}P < 0.01$, and $^{***}P < 0.01$ (means ± SEM).

(0.01 ± 0.01; $P = 0.03$), and nAG (0.003 ± 0.001; $P = 0.001$) (Fig. 5B). Accordingly, NCI-H295R cells transfected with *PRKACA* L206R (together with RIIβ) showed increased *CASP16P* mRNA expression compared with cells transfected with *PRKACA* WT (140 ± 15.8 versus 103 ± 10; $P < 0.05$) (Fig. 5C). Because activation of PKA with 8-Br-cAMP protected RIIβ from degradation, we tested whether CASP16P mRNA levels decrease with 8-Br-cAMP treatment. We observed a significant decrease in both PRKACA L206R (140 ± 15.8 versus 58.2 ± 7.7; $P < 0.01$)– and WT (103 ± 10 versus 47 ± 6.7; $P < 0.01$)–transfected NCI-H295R cells (Fig. 5C). In addition, 8-Br-cAMP significantly reduced CASP16P mRNA levels in untransfected NCI-H295R cells (108 ± 9.7 versus 53 ± 5.8; $P < 0.01$) (Fig. 5D). These in vitro and ex vivo results suggest involvement of CASP16P in RIIβ degradation. While reported as a gene in other mammals, CASP16P is listed in multiple databases (ENSEMBL: ENSG00000228146) as a pseudogene in humans despite having several characteristics of a real gene, including the presence of intronic sequences and a continuous open reading frame (ORF) that is very similar to its murine ortholog (fig. S6A). Overexpression of a hemagglutinin (HA)–tagged CASP16P in NCI-H295 cells showed that the protein is indeed translated. Moreover, that the effects seen in our previous experiments are likely directly mediated by the CASP16P protein and not its mRNA as CASP16P overexpression in NCI-H295R cells significantly decreased endogenous RIIβ levels (0.33 ± 0.17 versus 1 ± 0.12; $P < 0.05$) (Fig. 5, E and F). CASP16P overexpression had no impact on the other PKA regulatory subunits (Fig. 5E). Similar results were observed for the two human ACC cell lines CU-ACC1 and CU-ACC2 (fig. S7, A to D). In addition, phospho-RIIβ, the form sensitive to caspase degradation, was significantly reduced when CASP16P was overexpressed in the presence of Cα L206R (1 ± 0.002 versus 0.62 ± 0.03; $P < 0.01$) (fig. S6, B and C). These results suggest that CASP16P is a protein-encoding gene, and its increased expression in the presence of Cα L206R is likely responsible for RIIβ degradation.

DISCUSSION

A decrease in the PKA RIIβ subunit in a subgroup of CPA has long been demonstrated (*12*), and we could recently show this to be associated with *PRKACA* mutations (*13*). Here, we provide a direct link between the *PRKACA* L206R mutations and RIIβ loss. Although free R subunits are canonically degraded via the proteasome (*19*), our results indicate that active caspases, and not the proteasome, are responsible for RIIβ degradation in the presence of the Cα L206R mutation (Fig. 6). In Cα WT cells, RIIβ is not degraded, likely due to formation of a stable holoenzyme, masking the phosphoserine (S114) in the RIIβ inhibitory sequence (Fig. 6A). The constitutive activity of Cα L206R increases CASP16P mRNA, and because of the impaired binding of RIIβ to Cα L206R (*1*, *10*), phospho-S114 is unmasked, recognized, and cleaved by caspase 16 (Fig. 6B). In line with this model, when RIIβ does not contain a phosphoserine within its inhibitory site, it is not recognized for cleavage (Fig. 6D). Activation of endogenous, WT PKA by 8-Br-cAMP protects RIIβ degradation induced by the L206R mutant, likely via activation of one or more substrates that are not accessible to the L206R mutant, which has lost its normal interaction with R subunits and, hence, normal subcellular localization (Fig. 6, E and F).

In line with these observations, the simultaneous inhibition and activation of PKA activity with H89 or PKI and 8-Br-cAMP revealed a dominant effect of PKA inhibition over activation. This shows that inducing the PKA heterotetramer to dissociate is not the cause of RIIβ degradation. Simple binding of a cAMP analog was not sufficient to protect RIIβ from degradation either. At the same time, PKA Cα L206R activity is required for RIIβ degradation, as genetically inhibiting it by introducing a kinase-dead mutation (K73H) (*16*) into Cα L206R led to reduced RIIβ degradation (fig. S5, C and D). In contrast to RIIβ, RIα protein levels remained unaffected in the presence of Cα L206R, and this is because of the lack of a phosphosite in the inhibitory sequence of RIα (*20*, *21*). Caspases normally recognize and cleave proteins at a certain sequence containing the phosphomimetic amino acid aspartic acid but were also shown to often cleave proteins after a phosphorylated serine (*22*). Accordingly, the phosphorylation status of proteins was demonstrated to regulate their cleavage by caspases (*23*). In patient-derived adrenocortical adenoma tissues, only one caspase gene, CASP16P, was found overexpressed in *PRKACA*-mutated CPA compared with *PRKACA*-WT tumors, which was also up-regulated in cell culture when Cα L206R was present. CASP16P was considered to be a pseudogene (*24*); it is nonetheless transcribed and presumably translated (*25*). The ORF of CASP16P shows large areas of identity with its translated murine ortholog CASP16 (fig. S6A), suggesting that it might be itself translated. Transfection of a plasmid with the ORF sequence of CASP16P tagged with HA showed that CASP16P is translated and results in a stable protein. CASP16P overexpression induces degradation of endogenous RIIβ in NCI-H295R cells, whereas all other regulatory subunits remain largely unaffected (Fig. 5, E and F), confirming CASP16P involvement in RIIβ degradation and in line with the increased CASP16P mRNA levels in PKA-mutated CPA samples (*18*). We could demonstrate that this mechanism is also adrenal specific, as Cα L206R does not trigger RIIβ degradation in HEK293T or melanoma cells (fig. S2, E to M) but in three human ACC cell lines (Fig. 1, A and B, and fig. S2, A to D). Furthermore, we described already earlier *PRKACA*-mutated patient-derived tumor samples to have significantly decreased RIIβ protein levels compared with Cα WT tumors (*13*), at that time without explanation for this observation. Here, now, we could provide functional evidence to explain how *PRKACA* mutations, by up-regulating CASP16P levels, lead to RIIβ degradation in patient-derived tissues.

PKA specificity is regulated by AKAPs that bind the regulatory subunits of PKA and localize the whole heterotetramer to different subcellular compartments, where it forms multivalent protein complexes (*26*, *27*). Our LC-MS/MS analyses in NCI-H295R cells also identified potential RIIβ interaction partners in the presence of the Cα L206R mutant. AKAP2, TBC1D4 [a RAB-GTPase activating protein (GAP)], and PCYT1A (an enzyme involved in phosphatidylcholine synthesis) were initially good candidates but were excluded from further investigation after co-IP and WB verification (fig. S8, A and B). Under unstimulated conditions, the protein golgin A3 only interacted with unphosphorylated RIIβ in the presence of Cα L206R (fig. S8, C and D). Golgin A3 is localized at the cytoplasmic side of the Golgi apparatus (*28*) and contains several caspase recognition sites leading to its cleavage by different caspases during apoptosis (*29*). While knocking down *GOLGA3*, further reduced RIIβ-FLAG levels even in Cα WT–transfected cells (Fig. 6, A and C), golgin A3 overexpression, by acting as putative AKAP, stabilized RIIβ, likely by restoring PKA subunit localization. Golgin A3 was identified as the dynein-interacting protein that is responsible for proper Golgi positioning (*30*), and Golgi apparatus structure was previously shown

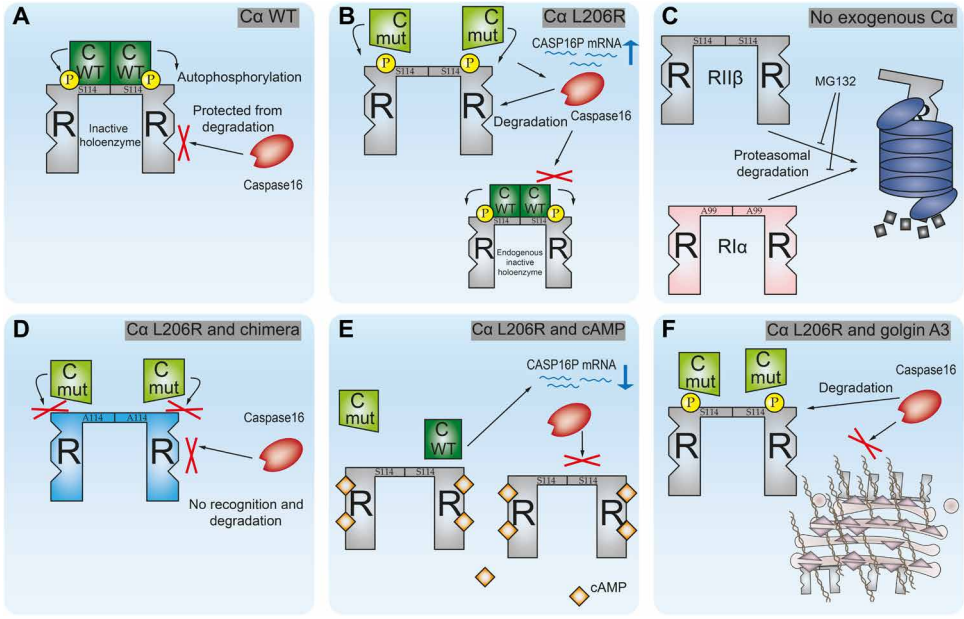

Fig. 6. Schematic representation showing the proposed mechanism of the fate of RIIβ in adrenocortical cells. Fate of RIIβ in the presence of (**A**) Cα WT or (**B**) the Cα L206R mutant. (**C**) Without any exogenous Cα, regulatory subunits are degraded via the proteasome. (**D**) nonphosphorylatable R subunits are not recognized by caspase 16. (**E**) 8-Br-cAMP, by activating the endogenous Ca WT and, hence, restoring physiological PKA signaling, reduces levels of CASP16P mRNA. (**F**) Overexpression of golgin A3 saves RIIβ from caspase 16–mediated cleavage.

to be dependent on PKA activity (*31*). This is in line with our own results showing Golgi apparatus delocalization in Cα L206R-mutated CPA (*13*) and underlines the importance of proper PKA subunit localization, which seems to be disrupted by Cα L206R.

There are also defects in other regulatory subunits of PKA associated with CS. Mutations in the regulatory subunit Iα resulting in a truncated RIα protein were identified as rare events in unilateral CPA (*32*); however, they are frequent in Carney complex (*33*). Copy number gains in the regulatory subunit Iβ have also been very recently identified in CPA (*34*). However, in the context of the mutations in the PKA catalytic subunit α, the loss of the regulatory subunit IIβ expression, as shown in this study, plays a relevant role in the defects in PKA signaling leading to cortisol oversecretion in CPA.

In conclusion, we show that in adrenal cells and tissue, the activity of the Cα mutant L206R triggers RIIβ degradation. Increased expression of CASP16P mRNA levels in Cα-mutated CPA and the activity of the overexpressed protein in vitro give strong evidence that CASP16P is responsible for RIIβ degradation. Our results additionally show the phosphorylation site within RIIβ's inhibitory site makes this subunit susceptible for caspase 16–mediated cleavage.

MATERIALS AND METHODS

Plasmids

Plasmids carrying human RIα, RIIβ, RIα-FLAG, RIIβ-FLAG, WT Cα, and Cα L206R sequences were described earlier (*11*). Point mutations were introduced into RIα-FLAG and RIIβ-FLAG plasmids with the Q5 Site-Directed Mutagenesis Kit (NEB). Mutagenesis primers were designed with the NEBaseChanger software tool. Five nanograms of template DNA was added to the reaction mix, and annealing occurred at 55°C. To generate RIIβ/RIα-inhibitory-FLAG and RIIβ/RIα-chimera-FLAG plasmids, restriction-free cloning was used. Primers, harboring the complete sequence to be replaced, were designed with the rf-cloning tool (www.rf-cloning.org). In a first PCR, 5 ng of each primer was used to generate the mega primers. During each of the five cycles, annealing occurred for 20 s in a ramp-wise manner, increasing the temperature for 0.5°C/s. Elongation time was 15 s. In the second PCR, 100 ng of the parental plasmid was added to the reaction mix of the first PCR, and annealing occurred at 62°C and elongation time was 12 min. All primer sequences are listed in table S2.

Design of HA-tagged CASP16P plasmid

The synthesis of the ORF of the CASP16P gene (ENSEMBL: ENSG00000228146) with the sequence for the HA tag (tatccatatgatgttccagattatgct) inserted at the N terminus was ordered from GeneArt service (a Life Technologies Company, Regensburg, Germany). The fragment was inserted into pcDNA3.1(+). The final construct was verified by sequencing. The sequence identity within the insertion sites was 100%.

Cell culture, transfections, and treatments

NCI-H295R and HEK293T cells were obtained from American Type Culture Collection (ATCC). NCI-H295R cells were cultured in Dulbecco's modified Eagle's medium (DMEM)/F12 supplemented with 1× insulin-transferrin-selenium and Nu-Serum (2.5%), and HEK293A cells were cultured in Dulbecco's Modified Eagle Medium (DMEM) (high glucose) supplemented with 10% fetal calf serum (FCS). Both cell lines were authentified by short tandem repeat (STR) analysis and tested regularly for mycoplasma contamination. For transfection, cells were seeded in 12-well plates (3×10^5 per well in 1 ml) or 15-cm dishes (9×10^6) for co-IPs 1 day before transfection. In total, 1 μg of DNA was diluted in 100 μl of OPTI-MEM and 3 μl of HP X-treme transfection reagent (Roche, Mannheim, Germany).

The transfection mix was incubated at room temperature (RT) for 20 min and subsequently added to cells. Lysates were harvested 96 hours after transfection. For gene knockdown, siRNA pools against *PRKAR2B*, *GOLGA3*, and ctrl (all Dharmacon, GE Healthcare) were diluted in serum-free media to achieve a final concentration of 1 μM, and lysates were harvested 96 hours after transfection. Cells were treated with chemicals for 24 hours (if not stated otherwise) at final concentrations of 10 μM MG-132, 20 μM H-89 (both Sigma-Aldrich, St. Louis, MO, USA), 1 mM 8-Br-cAMP, 10 μM Rp-8-Br-cAMPs, 10 μM Rp-8-PIP-cAMPs (all BioLog, Bremen, Germany), 60 μM Z-VAD-FMK (Merck Millipore, Darmstadt, Germany), 20 nM tautomycetin (for 96 hours) (Tocris Biosciences, USA), 20 μM st-Ht31, and st-Ht31P (Promega, Madison, WI, USA).

LC-MS/MS of steroid hormones

Steroid hormones in cell culture supernatants were quantified with the MassChrom steroids kit (Chromsystems) on a Qtrap 6500+ (Sciex) mass spectrometer coupled to a 1290 Infinity HPLC System (Agilent). Signal analysis was performed with Analyst Software (1.6.3, Sciex) as described elsewhere (*35*).

SDS–polyacrylamide gel electrophoresis and immunoblot

Cells were lysed in radioimmunoprecipitation assay buffer (Sigma-Aldrich) containing protease inhibitor (Sigma-Aldrich) and phosphatase inhibitor (Santa Cruz) cocktails. Ten micrograms of protein was loaded on a 4 to 15% denaturing gradient gel, and proteins were separated by SDS–polyacrylamide gel electrophoresis. Proteins were transferred by tank blot onto a polyvinylidene difluoride membrane that was subsequently blocked in 5% skimmed milk in tris-buffered saline (TBS)–Tween 20 buffer at RT for 1 hour. Primary antibodies (FLAG: Sigma-Aldrich, clone: F1804, 1:5000; *PRKACA*: BD Biosciences, #5B, 1:1000; *PRKAR2B*: BD Biosciences, #45, 1:1000; p-*PRKAR2B*: LSBio, #LS-C357179, 1:1000; GOLGA3: Novus, #NBP1-91952, 1:200; α-tubulin: Sigma-Aldrich, #T9026, 1:20000; and glyceraldehyde-3-phosphate dehydrogenase (GAPDH): Sigma-Aldrich, #g9549, 1:10,000) were incubated overnight (O/N) at 4°C. Membranes were washed three times in TBS–Tween 20 buffer, and horseradish peroxidase–labeled secondary antibodies (goat–anti-rabbit, Jackson ImmunoResearch Laboratories, #111-035-144, or goat–anti-mouse, Jackson ImmunoResearch Laboratories, #115-035-003, as appropriate) were diluted 1:10,000 and incubated at RT for 1 hour. The protein-antibody complex was visualized with enhanced chemiluminescence using Amersham ECL Prime reagent (GE Healthcare) and documented on an x-ray film (Fuji).

Coimmunoprecipitation

Cells were lysed 96 hours after transfection in IP lysis buffer (20 mM tris, 150 mM NaCl, 1 mM EDTA, 1 mM EGTA, and 0.1% NP-40) containing protease and phosphatase inhibitors and raised through a syringe for five times before cell debris was removed at >1100*g* at 4°C for 10 min. Supernatants were subsequently mixed with precoupled magnetic FLAG beads (Sigma-Aldrich) and incubated for 2 hours. Beads were collected with a magnet and washed five times with IP lysis buffer. To elute proteins from beads, beads were boiled in SDS-loading buffer, and the resulting proteins were subsequently loaded on a gel.

Identifying RIIβ interaction partners by nanoLC-MS/MS

NCI-H295R cells were transfected with Cα WT and RIIβ-FLAG or Cα L206R and RIIβ-FLAG, and co-IPs were performed as described above. To determine proteins bound unspecifically to FLAG beads, all transfections and conditions were additionally performed with untagged RIIβ plasmids.

In-solution digestion

Proteins were stored in 1× NuPage sample buffer, reduced in 50 μM dithiothreitol reducing reagent at 70°C for 10 min and alkylated with 120 mM iodoacetamide at RT in the dark for 20 min. Precipitation of proteins occurred O/N at −20°C with fourfold volume of acetone. Pellets were subsequently washed four times with ice-cold acetone. Precipitated proteins were then dissolved in 100 μl of 8 M urea in 100 mM ammonium bicarbonate and digested with 0.25 μg of Lys-C (Wako) at 30°C for 2 hours. Samples were subsequently diluted to 2 M urea by adding 300 μl of 100 mM ammonium bicarbonate. Trypsin (0.25 μg) was added, and digestion followed O/N at 37°C. Desalting of peptides occurred using C18 Stage Tips (*36*). Each stage tip was prepared with three discs of C18 Empore SPE Discs (3M) in a 200-μl pipet tip. Peptides were then eluted with 60% acetonitrile in 0.1% formic acid and dried in a vacuum concentrator (Eppendorf). Peptides were stored at −20°C and dissolved in 2% acetonitrile/0.1% formic acid before nanoLC-MS/MS analysis.

nanoLC-MS/MS analysis

NanoLC-MS/MS analyses were performed on an Orbitrap Fusion mass spectrometer (Thermo Fisher Scientific), equipped with an EASY-Spray Ion Source and coupled to an EASY-nLC 1000 liquid chomatograph (Thermo Fisher Scientific). Peptides were loaded on a trapping column and separated on an EASY-Spray column with a 140-min linear gradient from 3 to 45% acetonitrile and 0.1% formic acid. Both MS and MS/MS scans were acquired in the Orbitrap analyzer with a resolution of 15,000. Higher-energy collisional dissociation (HCD) with 35% normalized collision energy was applied. Top-speed data-dependent MS/MS method with a fixed cycle time of 3 s was used. Dynamic exclusion was applied with a repeat count of 1 and an exclusion duration of 60 s, and singly charged precursors were excluded from selection. Minimum signal threshold for precursor selection was set to 50,000. Predictive automatic gain control (pAGC) was used with a target value of 5×10^4 for MS/MS scans. EASY-IC was used for internal calibration.

Raw data processing and database search

For MS raw data file processing, database searches, and quantification, the MaxQuant version 1.5.7.4 was used (*37*). Search was performed against the *Homo sapiens* reference proteome database (Uniprot, download date 9 December 2016) and, in addition, against a database containing common cell culture contaminants. Search was performed with tryptic cleavage specificity with three allowed miscleavages. Less than 1% false discovery rate (FDR) on protein and peptide level was used for protein identification. In addition to default settings, protein N-terminal acetylation, Gln to pyro-Glu formation, and oxidation were included as variable modifications. For protein quantitation, the label free quantification (LFQ) intensities were used (*38*). Proteins with less than two identified razor/unique peptides were dismissed. Further data analysis steps were done with in-house–developed R scripts. For discrimination of unspecifically immunoprecipitated proteins, LFQ intensities of IP control samples were quantile normalized, and median intensities were calculated. Missing LFQ intensities in the pooled control samples were imputed with values close to the baseline. For comparison of experimental

conditions, missing values in one of the compared conditions were imputed. Data imputation was performed with values from a standard normal distribution with a mean of the 5% quantile of the combined $\log_{10}$-transformed LFQ intensities and an SD of 0.1. For the identification of significantly coimmunoprecipitated proteins, boxplot outliers were identified in intensity bins of at least 300 proteins. Log_2-transformed protein ratios IP versus ctrl with values outside a 1.5× (potential) or 3× (extreme) interquartile range (IQR) of the first or third quartile, respectively, were considered significantly coprecipitated. The underlying distribution was a mirrored distribution of the negative $\log_2$ ratios IP versus ctrl. For comparisons of replicate experiments and further analysis, protein intensity ratios were quantile normalized. The identification of significantly enriched proteins within replicate experiments and between experimental conditions was additionally done with the R package limma (*39*), and proteins with ratios in at least two biological replicates were considered significantly enriched with a Benjamini-Hochberg adjusted *P* value of 0.02 or lower, which corresponds to a *q* value of 2% (FDR).

Pulse chase experiments

NCI-H295R cells were washed twice with DPBS before starving media [DMEM/F12 supplemented with 1× ITS (insulin-transferrin-selenium), Gibco, life technologies] were added. Cells were incubated for 1 hour under starving conditions. Starving media were removed, and cells were incubated with pulse media [DMEM/F12 supplemented with 1× ITS +35S-labeled amino acids (methionine and cysteine) (PerkinElmer)] for 1 hour. Pulse media were removed, and cells were harvested in IP lysis buffer and IP was performed with magnetic FLAG beads as described above. Eluted proteins were loaded on a 12% polyacrylamide gel, and gels were dried afterward at 80°C for 1 hour in a gel dryer (Bio-Rad). Analysis of dried gels occurred by autoradiography on an x-ray film for 3 days.

RNA sequencing

Gene expression profile investigated by RNA sequencing was available for a large set of fresh-frozen adrenocortical tumors from a previous multicenter study coordinated by our group on behalf of the European Network for the Study of Adrenal Tumors (ENSAT) (*18*). In particular, this cohort included 52 adenomas (9 endocrine inactive, EIAs, and 43 CPA) and 7 carcinomas (ACC), while 4 nAGs were used as reference. The genetic background of adenomas was known from previous whole-exome sequencing (*4*) or Sanger sequencing for *PRKACA* mutation (*3*).

In brief, RNA was isolated by RNEasy Lipid Tissue Mini Kit (Qiagen, Hilden, Germany) (n = 23) or by Maxwell 16 Total RNA Purification Kit used with the Maxwell 16 Instrument (n = 36), according to the manufacturers' instruction. RNA quality control was performed by an Agilent Technologies 2100 Bioanalyzer, and an RNA integrity number (RIN) value ≥8 was required to ensure efficient mRNA sequencing. TruSeq RNA Library Prep Kit was applied before Illumina sequencing (NextSeq500) of pooled normalized libraries. Specifically, a paired-end 75–nucleotide (nt) mode (high-output flow cells) was used for a minimum of 40 to 100 million reads per sample.

An initial quality assessment was performed using FastQC v0.11.5 (www.bioinformatics.babraham.ac.uk/projects/fastqc). Adapter and quality trimming was done with Cutadapt, v1.1.5 (https://cutadapt.readthedocs.io/en/stable/). STAR v2.5.3a (*40*) was used to map the trimmed reads to the GENCODE human reference genome GRCh37 release 29. We used Samtools v1.3 (*41*) using htslib v1.3 for sam-to-bam-conversions as well as sorting and indexing of the alignment files. For gene annotation, the GENCODE human reference genome GRCh37 release 29 was used. FPKM (fragments per kilobase million) values and differential gene expression were calculated with Cufflinks package v2.2.1 (*42*). Only FPKM values of all genes with a coefficient of variation ≥0.5 were used in the evaluation.

Tissue collection for RT-qPCR

Fresh tumor samples from 34 patients who underwent surgery for adrenal tumors were collected as part of the ENSAT registry and biobank (https://registry.ensat.org), conformed to the principles of the Declaration of Helsinki, the Good Clinical Practice Guidelines, and was approved by the ethics committee of the University of Würzburg (approval # 86/03 and 88/11), and all patients provided informed consent. nAGs were collected from patients who underwent adrenalectomy due to renal cancer (n = 16). After surgery, fat and connective tissue were removed, and tissues were immediately snap frozen in liquid nitrogen and stored at −80°C until RNA were extracted.

RNA extraction and RT-qPCR

RNA from fresh-frozen tissues or transfected NCI-H295R cells was isolated using the RNeasy Lipid Tissue Mini Kit (Qiagen) and reverse transcribed with the QuantiTect Reverse Transcription Kit (Qiagen). CASP16P RT-qPCR was performed using predesigned TaqMan gene expression probes (Thermo Fisher Scientific) for CASP16P (*Hs00395216_m1*) and beta actin (ACTB) (Hs9999903_m1) were used for normalization. Five nanograms of cDNA was used for each PCR, and each sample was analyzed in duplicate. Transcripts were amplified using the TaqMan Gene Expression Master Mix (Thermo Fisher Scientific), the CFX96 real-time thermocycler (Bio-Rad), and Bio-Rad CFX Manager 2.0 software. Cycling conditions were 95°C for 3 min followed by 50 cycles of 95°C for 30 s, 60°C for 30 s, and 72°C for 30 s. Gene expression levels were normalized to those of ACTB by using the ΔCT method (*43*).

Statistical analyses

One-way analysis of variance (ANOVA) with either Tukey's or Dunn's posttest or Kruskal-Wallis test was used to determine statistically significant differences between more than two parametric and nonparametric datasets, respectively. To determine the significant differences between two nonparametric datasets, unpaired *t* test was used. Statistical analyses were performed using GraphPad Prism (version 6.0). For normal distribution testing, Kolmogorov-Smirnov test was used. $P < 0.05$ was considered as statistically significant.

SUPPLEMENTARY MATERIALS

Supplementary material for this article is available at http://advances.sciencemag.org/cgi/content/full/7/8/eabd4176/DC1

View/request a protocol for this paper from *Bio-protocol*.

REFERENCES AND NOTES

1. F. Beuschlein, M. Fassnacht, G. Assie, D. Calebiro, C. A. Stratakis, A. Osswald, C. L. Ronchi, T. Wieland, S. Sbiera, F. R. Faucz, K. Schaak, A. Schmittfull, T. Schwarzmayr, O. Barreau, D. Vezzosi, M. Rizk-Rabin, U. Zabel, E. Szarek, P. Salpea, A. Forlino, A. Vetro, O. Zuffardi, C. Kisker, S. Diener, T. Meitinger, M. J. Lohse, M. Reincke, J. Bertherat, T. M. Strom,

B. Allolio, Constitutive activation of PKA catalytic subunit in adrenal Cushing's syndrome. *N. Engl. J. Med.* **370**, 1019–1028 (2014).
2. G. Goh, U. I. Scholl, J. M. Healy, M. Choi, M. L. Prasad, C. Nelson-Williams, J. W. Kunstman, R. Korah, A. C. Suttorp, D. Dietrich, M. Haase, H. S. Willenberg, P. Stalberg, P. Hellman, G. Akerstrom, P. Bjorklund, T. Carling, R. P. Lifton, Recurrent activating mutation in PRKACA in cortisol-producing adrenal tumors. *Nat. Genet.* **46**, 613–617 (2014).
3. G. Di Dalmazi, C. Kisker, D. Calebiro, M. Mannelli, L. Canu, G. Arnaldi, M. Quinkler, N. Rayes, A. Tabarin, M. Laure Jullie, F. Mantero, B. Rubin, J. Waldmann, D. K. Bartsch, R. Pasquali, M. Lohse, B. Allolio, M. Fassnacht, F. Beuschlein, M. Reincke, Novel somatic mutations in the catalytic subunit of the protein kinase A as a cause of adrenal Cushing's syndrome: A European multicentric study. *J. Clin. Endocrinol. Metab.* **99**, E2093–E2100 (2014).
4. C. L. Ronchi, G. Di Dalmazi, S. Faillot, S. Sbiera, G. Assie, I. Weigand, D. Calebiro, T. Schwarzmayr, S. Appenzeller, B. Rubin, J. Waldmann, C. Scaroni, D. K. Bartsch, F. Mantero, M. Mannelli, D. Kastelan, I. Chiodini, J. Bertherat, M. Reincke, T. M. Strom, M. Fassnacht, F. Beuschlein; European Network for the Study of Adrenocortical Tumors, Genetic landscape of sporadic unilateral adrenocortical adenomas without PRKACA p. Leu206Arg mutation. *J. Clin. Endocrinol. Metab.* **101**, 3526–3538 (2016).
5. S. S. Taylor, R. Ilouz, P. Zhang, A. P. Kornev, Assembly of allosteric macromolecular switches: lessons from PKA. *Nat. Rev. Mol. Cell Biol.* **13**, 646–658 (2012).
6. S. H. Francis, J. D. Corbin, Cyclic nucleotide-dependent protein kinases: Intracellular receptors for cAMP and cGMP action. *Crit. Rev. Clin. Lab. Sci.* **36**, 275–328 (1999).
7. B. S. Skalhegg, K. Tasken, Specificity in the cAMP/PKA signaling pathway. Differential expression, regulation, and subcellular localization of subunits of PKA. *Front. Biosci.* **5**, D678–D693 (2000).
8. M. Diskar, H. M. Zenn, A. Kaupisch, A. Prinz, F. W. Herberg, Molecular basis for isoform-specific autoregulation of protein kinase A. *Cell. Signal.* **19**, 2024–2034 (2007).
9. S. S. Taylor, J. A. Buechler, W. Yonemoto, cAMP-dependent protein kinase: Framework for a diverse family of regulatory enzymes. *Annu. Rev. Biochem.* **59**, 971–1005 (1990).
10. D. Calebiro, A. Hannawacker, S. Lyga, K. Bathon, U. Zabel, C. Ronchi, F. Beuschlein, M. Reincke, K. Lorenz, B. Allolio, C. Kisker, M. Fassnacht, M. J. Lohse, PKA catalytic subunit mutations in adrenocortical Cushing's adenoma impair association with the regulatory subunit. *Nat. Commun.* **5**, 5680 (2014).
11. K. Bathon, I. Weigand, J. T. Vanselow, C. L. Ronchi, S. Sbiera, A. Schlosser, M. Fassnacht, D. Calebiro, Alterations in protein kinase A substrate specificity as a potential cause of cushing syndrome. *Endocrinology* **160**, 447–459 (2019).
12. C. Vincent-Dejean, L. Cazabat, L. Groussin, K. Perlemoine, G. Fumey, F. Tissier, X. Bertagna, J. Bertherat, Identification of a clinically homogenous subgroup of benign cortisol-secreting adrenocortical tumors characterized by alterations of the protein kinase A (PKA) subunits and high PKA activity. *Eur. J. Endocrinol.* **158**, 829–839 (2008).
13. I. Weigand, C. L. Ronchi, M. Rizk-Rabin, G. D. Dalmazi, V. Wild, K. Bathon, B. Rubin, D. Calebiro, F. Beuschlein, J. Bertherat, M. Fassnacht, S. Sbiera, Differential expression of the protein kinase A subunits in normal adrenal glands and adrenocortical adenomas. *Sci. Rep.* **7**, 49 (2017).
14. K. Kiseljak-Vassiliades, Y. Zhang, S. M. Bagby, A. Kar, N. Pozdeyev, M. Xu, K. Gowan, V. Sharma, C. D. Raeburn, M. Albuja-Cruz, K. L. Jones, L. Fishbein, R. E. Schweppe, H. Somerset, T. M. Pitts, S. Leong, M. E. Wierman, Development of new preclinical models to advance adrenocortical carcinoma research. *Endocr. Relat. Cancer* **25**, 437–451 (2018).
15. A. Godbole, S. Lyga, M. J. Lohse, D. Calebiro, Internalized TSH receptors en route to the TGN induce local G_s-protein signaling and gene transcription. *Nat. Commun.* **8**, 443 (2017).
16. G. H. Iyer, S. Garrod, V. L. Woods Jr., S. S. Taylor, Catalytic independent functions of a protein kinase as revealed by a kinase-dead mutant: Study of the Lys72His mutant of cAMP-dependent kinase. *J. Mol. Biol.* **351**, 1110–1122 (2005).
17. D. W. Carr, Z. E. Hausken, I. D. Fraser, R. E. Stofko-Hahn, J. D. Scott, Association of the type II cAMP-dependent protein kinase with a human thyroid RII-anchoring protein. Cloning and characterization of the RII-binding domain. *J. Biol. Chem.* **267**, 13376–13382 (1992).
18. G. Di Dalmazi, B. Altieri, C. Scholz, S. Sbiera, M. Luconi, J. Waldman, D. Kastelan, F. Ceccato, I. Chiodini, G. Arnaldi, A. Riester, A. Osswald, F. Beuschlein, S. Sauer, M. Fassnacht, S. Appenzeller, C. L. Ronchi, RNA-sequencing and somatic mutation status of adrenocortical tumors: Novel pathogenetic insights. *J. Clin. Endocrinol. Metab.* **105**, dgaa616 (2020).
19. A. N. Hegde, A. L. Goldberg, J. H. Schwartz, Regulatory subunits of cAMP-dependent protein kinases are degraded after conjugation to ubiquitin: A molecular mechanism underlying long-term synaptic plasticity. *Proc. Natl. Acad. Sci. U.S.A.* **90**, 7436–7440 (1993).
20. J. Kuret, K. E. Johnson, C. Nicolette, M. J. Zoller, Mutagenesis of the regulatory subunit of yeast cAMP-dependent protein kinase. Isolation of site-directed mutants with altered binding affinity for catalytic subunit. *J. Biol. Chem.* **263**, 9149–9154 (1988).
21. A. Budillon, A. Cereseto, A. Kondrashin, M. Nesterova, G. Merlo, T. Clair, Y. S. Cho-Chung, Point mutation of the autophosphorylation site or in the nuclear location signal causes protein kinase A RII beta regulatory subunit to lose its ability to revert transformed fibroblasts. *Proc. Natl. Acad. Sci. U.S.A.* **92**, 10634–10638 (1995).
22. J. E. Seaman, O. Julien, P. S. Lee, T. J. Rettenmaier, N. D. Thomsen, J. A. Wells, Cacidases: Caspases can cleave after aspartate, glutamate and phosphoserine residues. *Cell Death Differ.* **23**, 1717–1726 (2016).
23. J. Walter, A. Schindzielorz, J. Grunberg, C. Haass, Phosphorylation of presenilin-2 regulates its cleavage by caspases and retards progression of apoptosis. *Proc. Natl. Acad. Sci. U.S.A.* **96**, 1391–1396 (1999).
24. M. Centola, X. Chen, R. Sood, Z. Deng, I. Aksentijevich, T. Blake, D. O. Ricke, X. Chen, G. Wood, N. Zaks, N. Richards, D. Krizman, E. Mansfield, S. Apostolou, J. Liu, N. Shafran, A. Vedula, M. Hamon, A. Cercek, T. Kahan, D. Gumucio, D. F. Callen, R. I. Richards, R. K. Moyzis, N. A. Doggett, F. S. Collins, P. P. Liu, N. Fischel-Ghodsian, D. L. Kastner, Construction of an approximately 700-kb transcript map around the familial Mediterranean fever locus on human chromosome 16p13.3. *Genome Res.* **8**, 1172–1191 (1998).
25. L. Eckhart, C. Ballaun, M. Hermann, J. L. VandeBerg, W. Sipos, A. Uthman, H. Fischer, E. Tschachler, Identification of novel mammalian caspases reveals an important role of gene loss in shaping the human caspase repertoire. *Mol. Biol. Evol.* **25**, 831–841 (2008).
26. V. M. Coghlan, B. A. Perrino, M. Howard, L. K. Langeberg, J. B. Hicks, W. M. Gallatin, J. D. Scott, Association of protein kinase A and protein phosphatase 2B with a common anchoring protein. *Science* **267**, 108–111 (1995).
27. T. M. Klauck, M. C. Faux, K. Labudda, L. K. Langeberg, S. Jaken, J. D. Scott, Coordination of three signaling enzymes by AKAP79, a mammalian scaffold protein. *Science* **271**, 1589–1592 (1996).
28. J. I. Sbodio, S. W. Hicks, D. Simon, C. E. Machamer, GCP60 preferentially interacts with a caspase-generated golgin-160 fragment. *J. Biol. Chem.* **281**, 27924–27931 (2006).
29. M. Mancini, C. E. Machamer, S. Roy, D. W. Nicholson, N. A. Thornberry, L. A. Casciola-Rosen, A. Rosen, Caspase-2 is localized at the Golgi complex and cleaves golgin-160 during apoptosis. *J. Cell Biol.* **149**, 603–612 (2000).
30. S. Yadav, M. A. Puthenveedu, A. D. Linstedt, Golgin160 recruits the dynein motor to position the Golgi apparatus. *Dev. Cell* **23**, 153–165 (2012).
31. F. Mavillard, J. Hidalgo, D. Megias, K. L. Levitsky, A. Velasco, PKA-mediated Golgi remodeling during cAMP signal transmission. *Traffic* **11**, 90–109 (2010).
32. J. Bertherat, L. Groussin, F. Sandrini, L. Matyakhina, T. Bei, S. Stergiopoulos, T. Papageorgiou, I. Bourdeau, L. S. Kirschner, C. Vincent-Dejean, K. Perlemoine, C. Gicquel, X. Bertagna, C. A. Stratakis, Molecular and functional analysis of PRKAR1A and its locus (17q22-24) in sporadic adrenocortical tumors: 17q losses, somatic mutations, and protein kinase A expression and activity. *Cancer Res.* **63**, 5308–5319 (2003).
33. R. Correa, P. Salpea, C. A. Stratakis, Carney complex: An update. *Eur. J. Endocrinol.* **173**, M85–M97 (2015).
34. L. Drougat, N. Settas, C. L. Ronchi, K. Bathon, D. Calebiro, A. G. Maria, S. Haydar, A. Voutetakis, E. London, F. R. Faucz, C. A. Stratakis, Genomic and sequence variants of protein kinase A regulatory subunit type 1β (PRKAR1B) in patients with adrenocortical disease and Cushing syndrome. *Genet. Med.* **23**, 174–182 (2021).
35. S. Schweitzer, M. Kunz, M. Kurlbaum, J. Vey, S. Kendl, T. Deutschbein, S. Hahner, M. Fassnacht, T. Dandekar, M. Kroiss, Plasma steroid metabolome profiling for the diagnosis of adrenocortical carcinoma. *Eur. J. Endocrinol.* **180**, 117–125 (2019).
36. J. Rappsilber, Y. Ishihama, M. Mann, Stop and go extraction tips for matrix-assisted laser desorption/ionization, nanoelectrospray, and LC/MS sample pretreatment in proteomics. *Anal. Chem.* **75**, 663–670 (2003).
37. J. Cox, M. Mann, MaxQuant enables high peptide identification rates, individualized p.p.b.-range mass accuracies and proteome-wide protein quantification. *Nat. Biotechnol.* **26**, 1367–1372 (2008).
38. J. Cox, M. Y. Hein, C. A. Luber, I. Paron, N. Nagaraj, M. Mann, Accurate proteome-wide label-free quantification by delayed normalization and maximal peptide ratio extraction, termed MaxLFQ. *Mol. Cell. Proteomics* **13**, 2513–2526 (2014).
39. M. E. Ritchie, B. Phipson, D. Wu, Y. Hu, C. W. Law, W. Shi, G. K. Smyth, *limma* powers differential expression analyses for RNA-sequencing and microarray studies. *Nucleic Acids Res.* **43**, e47 (2015).
40. A. Dobin, C. A. Davis, F. Schlesinger, J. Drenkow, C. Zaleski, S. Jha, P. Batut, M. Chaisson, T. R. Gingeras, STAR: Ultrafast universal RNA-seq aligner. *Bioinformatics* **29**, 15–21 (2013).
41. H. Li, B. Handsaker, A. Wysoker, T. Fennell, J. Ruan, N. Homer, G. Marth, G. Abecasis, R. Durbin; 1000 Genome Project Data Processing Subgroup, The sequence alignment/map format and SAMtools. *Bioinformatics* **25**, 2078–2079 (2009).
42. C. Trapnell, B. A. Williams, G. Pertea, A. Mortazavi, G. Kwan, M. J. van Baren, S. L. Salzberg, B. J. Wold, L. Pachter, Transcript assembly and quantification by RNA-Seq reveals unannotated transcripts and isoform switching during cell differentiation. *Nat. Biotechnol.* **28**, 511–515 (2010).
43. M. W. Pfaffl, A new mathematical model for relative quantification in real-time RT-PCR. *Nucleic Acids Res.* **29**, e45 (2001).

Acknowledgments: We thank H. Urlaub for expert technical assistance. SK-MEL-28 and A375 human melanoma cell lines were provided by J. P. Friedmann Angeli, and the adrenocortical cell lines CU-ACC1 and CU-ACC2 were provided by K. Kiseljak-Vassiliades. **Funding:** This study was supported by the IZKF Würzburg (grant B-281 to D.C. and M.F.), the ERA-NET "E-Rare" (grant 01GM1407B to M.F. and D.C.), the Else Kröner-Fresenius-Stiftung (grant 2016_A96 to S.S. and M.K.), and the DFG German Research Foundation (grant KR-4371/1-2 to M.K., FA-466/4-2 and FA-466/8-1 to M.F., SB52/1-1 to S.S., and RO-5435/3-1 to C.L.R.) and project 314061271-TRR 205. K.B. was supported by a grant of the German Excellence Initiative to the Graduate School of Life Sciences, University of Würzburg. This publication was supported by the Open Access Publication Fund of the University of Würzburg. **Author contributions:** I.W., M.F., D.C., and S.S. designed the study; I.W., J.T.V., K.B., K.L., and S.H. performed experiments; I.W., C.L.R., J.T.V., A.S., M.K., M.F., D.C., and S.S. analyzed the data; I.W., M.F., D.C., and S.S. wrote the manuscript. All authors read the manuscript and critically revised it. **Competing interests:** The authors declare that they have no competing interests. **Data and materials availability:** All data needed to evaluate the conclusions in the paper are present in the paper and/or the Supplementary Materials. Proteomics data obtained from nanoLC-MS/MS will be deposited on the OSF platform. Additional data related to this paper may be requested from the authors.

Submitted 23 June 2020
Accepted 6 January 2021
Published 19 February 2021
10.1126/sciadv.abd4176

Citation: I. Weigand, C. L. Ronchi, J. T. Vanselow, K. Bathon, K. Lenz, S. Herterich, A. Schlosser, M. Kroiss, M. Fassnacht, D. Calebiro, S. Sbiera, PKA Cα subunit mutation triggers caspase-dependent RIIβ subunit degradation via Ser^{114} phosphorylation. *Sci. Adv.* **7**, eabd4176 (2021).

ScienceAdvances

PKA C# subunit mutation triggers caspase-dependent RII# subunit degradation via Ser phosphorylation

Isabel WeigandCristina L. RonchiJens T. VanselowKerstin BathonKerstin LenzSabine HerterichAndreas SchlosserMatthias KroissMartin FassnachtDavide CalebiroSilviu Sbiera

Sci. Adv., 7 (8), eabd4176. • DOI: 10.1126/sciadv.abd4176